

# Optical response of small closed-shell sodium clusters

George Pal

Physikalisch-Technische Bundesanstalt (PTB), Bundesallee 100, 38116 Braunschweig, Germany

Georgios Lefkidis, Hans Christian Schneider, and Wolfgang Hubner

Physics Department and Research Center OPTIMAS,

University of Kaiserslautern, P.O. Box 3049, 67653 Kaiserslautern, Germany

(Dated: February 22, 2024)

Absorption spectra of closed-shell  $\text{Na}_2$ ,  $\text{Na}_3^+$ ,  $\text{Na}_4$ ,  $\text{Na}_5^+$ ,  $\text{Na}_6$ ,  $\text{Na}_7^+$ , and  $\text{Na}_8$  clusters are calculated using a recently implemented conserving linear response method. In the framework of a quasiparticle approach, we determine electron-hole correlations in the presence of an external field. The calculated results are in excellent agreement with experimental spectra, and some possible cluster geometries that occur in experiments are analyzed. The position and the broadening of the resonances in the spectra arise from a consistent treatment of the scattering and dephasing contributions in the linear response calculation. Comparison between the experimental and the theoretical results yields information about the cluster geometry, which is not accessible experimentally.

PACS numbers: 78.67.-n Optical properties of low-dimensional, mesoscopic, and nanoscale materials and structures; 36.40.Vz Optical properties of clusters; 73.22.-f Electronic structure of nanoscale materials and related systems; 36.40.Cg Electronic and magnetic properties of clusters

## I. INTRODUCTION

The electronic configuration of small metal clusters is closely connected with their geometrical, chemical and optical properties<sup>1</sup>. Different aspects of this interrelation for small metal clusters have been extensively studied experimentally<sup>2(12)</sup> and theoretically<sup>13(34)</sup>. For instance, the measured photoabsorption cross section of mass-selected clusters yields important information about the interplay between the underlying nuclear configuration and the electronic structure. However, the geometry of the clusters in the gas phase is not directly accessible in experiments. *Ab initio* theory can help to determine the structures by choosing, among many possibilities, the most stable geometrical configuration, for which the calculated absorption spectrum is in good agreement with the experimental results.

Early theoretical attempts to understand the nature of electronic correlation in small alkali metal clusters are based on the shell<sup>3</sup> and density functional theory (DFT)-based jellium<sup>14(17)</sup> models. Quantum molecular approaches based on the Configuration Interaction (CI) procedures are powerful theoretical tools capable of yielding accurate electronic excited states and important information about the nature of the optically allowed transitions between them. The multi-reference single and double excitation CI has been successfully used to account for the dominant features of the absorption spectra of small sodium clusters<sup>19(23)</sup>, calculated from the oscillator strength of the transitions between the ground and the excited states. Also, time-dependent (TD) DFT methods are widely employed to compute the photoabsorption cross sections of small metal clusters, with various levels of sophistication for the exchange-correlation functional<sup>24(29)</sup>. A different way to compute optical spectra is to make use of the quasiparticle picture, where

a typical photoabsorption process involves an incoming photon and the transition of an electron from an occupied to an empty quasiparticle state. The determination of the cross section can be achieved by a calculation of a generalized \four-point\ (i.e., two-particle) electron-hole correlation function, which obeys a Bethe-Salpeter equation (BSE)<sup>30(34)</sup>. In practice, this is usually done in a two-step calculation: first the DFT or Hartree-Fock (HF) single-particle states are used as input into a GW-like procedure to obtain the quasiparticle corrections to the Kohn-Sham or HF ground-state eigenvalues<sup>35,36</sup>. Then a two-particle BSE effective equation with a screened direct and an unscreened exchange electron-hole interaction is solved. While the first step properly describes charged excitations (i.e., electron removal or addition, specific to direct or inverse photoelectron experiments), the second step accounts for neutral excitations (i.e., electron-hole pair creation, specific to photoabsorption experiments). A comprehensive comparison between the TDDFT and the GW + BSE approaches can be found in Ref. 32. To facilitate the numerical procedure, the screened Coulomb interaction, which is obtained in the GW step and which enters the BSE, is most often taken to be the statically screened Coulomb interaction. This simplification allows one to cast the effective two-particle BSE in the form of an energy-independent eigenvalue problem, which yields the excited states corresponding to neutral excitations of the system. As in the case of CI, the optical absorption cross section is then determined by the oscillator strengths of the transitions to the excited states, and a phenomenological parameter for the resonance peak broadening is added in order to compare the calculated spectra with the shapes of the experimental peaks. This phenomenological time for the individual transition mimics the combination of thermal broadening and electron lifetime.



stress that introducing a fixed quasiparticle lifetime for the calculation of  $\chi^r$  does not mean that the broadening of the resonances in  $\chi^r$  is given by this value. Rather, the resonance broadening, which is responsible for the finite width of the peaks in the absorption spectrum, is due to the imaginary part of the full correlation contribution  $\chi^r$ . The real part of  $\chi^r$  yields the shift in the resonance energies. Both effects, renormalization and broadening of the  $\chi^r$  spectrum, are thus related.

Equation 3 for the electron-hole correlation can be solved at different levels of approximation. Neglecting all Coulomb interactions and setting

$$\langle n_1 n_2 j | \chi^r | n_3 n_4 i \rangle = \langle n_1 n_3 | n_2 n_4 \rangle \quad (6)$$

one obtains for  $\chi^r$  the independent particle (Lindhard) result

$$\langle n_1 n_2 j | \chi^r | n_3 n_4 i \rangle = \frac{\langle n_1 n_3 | n_2 n_4 \rangle (f_{n_1} - f_{n_2})}{\sim (1 + i) \left( \frac{1}{n_1} + \frac{1}{n_2} \right)} : \quad (7)$$

Including direct Coulomb matrix elements, exchange elements and correlation contributions in that order, Eq. (3) resembles a BSE in the ladder approximation (denoted by BS-L in the following) plus exchange (BS-LX) and correlation terms (BS-LXC), respectively<sup>38</sup>. Recall that we use loosely here the term BSE for Eq. (3), even though the BSE is usually written for the four-point generalization of .

### III. PHOTOABSORPTION SPECTRA OF SMALL NA CLUSTERS

In this section we discuss photoabsorption spectra of closed-shell  $\text{Na}_2$ ,  $\text{Na}_3^+$ ,  $\text{Na}_4$ ,  $\text{Na}_5^+$ ,  $\text{Na}_6$ ,  $\text{Na}_7^+$ , and  $\text{Na}_8$  clusters. The numerical results are calculated according to Eq. (2) and compared with experiment. We choose clusters with closed-shell configurations with an even number of electrons, for which all molecular orbitals are doubly occupied or empty. Moreover,  $\text{Na}_2$ ,  $\text{Na}_3^+$ , and  $\text{Na}_8$  are magic-number clusters, for which the number of valence electrons equals the spherical-shell closing numbers 2 and 8, respectively<sup>6</sup>. The electron-hole correlation function is determined by solving Eq. (3) with the correlation kernel (4).

To obtain the equilibrium ( $T = 0\text{K}$ ) geometrical configuration, we perform a structural optimization using the HF approximation, which yields the single-particle ground state energies and wave functions. For the Na atoms we use the lanl2dz basis set (double-zeta set with relativistic Los Alamos effective core potential)<sup>42</sup>, in which the  $3s^1$  valence electron of each Na atom is represented by contracted Gaussian-like atomic orbitals (3s3p/2s2p) while the contribution of the core electrons is treated using effective core potentials (ECP). To test the stability of our results with respect to the basis set used in the calculations, we have also performed calculations with six other basis sets:

SHC (Goddard/Smalley ECP)<sup>43</sup>, CEP-4G (minimal set and Stephens/Basch/Krauss ECP), CEP-31G (split valence set) and CEP-121G (triple-split basis set)<sup>44</sup>, LanL2MB (MBS set and Los Alamos ECP)<sup>42</sup>, and SD-Dall (double-zeta set and Stuttgart/Dresden ECP)<sup>45</sup>. For larger basis sets such as lanl2dz, SHC, CEP-121G and SD-Dall the Na-Na distances vary by less than 1% at the end of the geometry optimization, and the peak positions of the absorption spectra differ by less than 0.1 eV. For smaller basis sets the Na-Na distances vary at most by 0.3 Å while the peak positions have deviations of less than 0.3 eV. Overall, a good comparison with experiment is found for lanl2dz, and in the following we refer only to results obtained using this basis set. When the absorption spectra are calculated from the density-density correlation function obtained in the Lindhard, BS-L and BS-LX approximations, we use a constant broadening  $\gamma = 0.03\text{ eV}$  in Eq. (6). When correlation terms are included in the calculations we use for the quasiparticle inverse lifetime the value  $\gamma = 0.15\text{ eV}$  in Eq. (4).

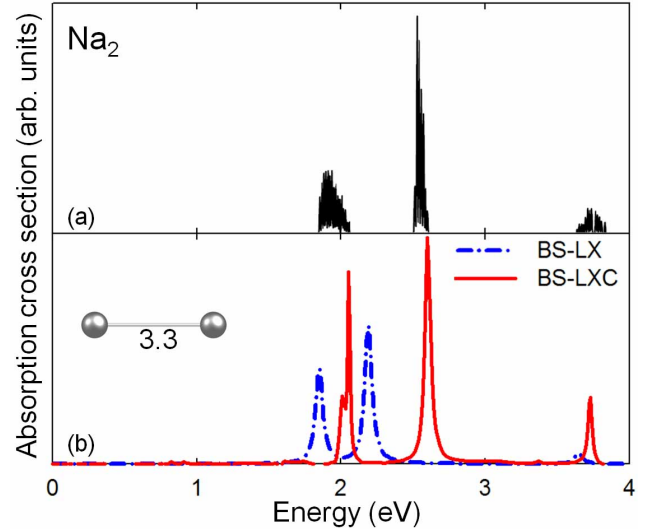


FIG. 1. Experimental and calculated absorption spectra of  $\text{Na}_2$ . (a) Experimental spectrum adapted from Ref. 46. (b) Cross section calculated from  $\chi^r$  in the BS-LXC (solid line) and BS-LX (dot-dashed) approximation. The inset shows the cluster structure with the distance in Å.

Within the present approach, the computed spectra should fulfill the f-sum rule for finite systems

$$\sum_Z \langle d | \hat{P} | n_1 \dots n_4 \rangle \frac{1}{3} \langle \hat{P} | n_1 n_2 d | n_3 n_4 \rangle = \sum_{x,y,z} \langle d | \hat{P} | n_1 n_2 d | n_3 n_4 \rangle \quad (8)$$

$$\text{Im} \langle n_2 n_1 j | \chi^r | n_3 n_4 i \rangle = \frac{\hbar^2}{m} N_e$$

for the conserving BS-LX and BS-LXC approximations. Here,  $m$  is the electron mass and  $N_e$  is the total number of electrons in the system. Equation (8) is equivalent to the Thomas-Reiche-Kuhn sum rule for the absorption cross section and is directly related to the particle number

conservation law<sup>38</sup>. For our results, Eq. (8) is numerically checked and the  $f$ -sum rule is fulfilled to better than 99%.

Calculated photoabsorption spectra for  $\text{Na}_2$  are shown in Fig. 1 and compared to experimental data. Only when correlations are included in the computation of  $\chi$ , the theoretical spectrum reproduces the experimental absorption peaks which occur around 1.97, 2.55, and 3.75 eV. The pronounced difference between the BS-LX and the BS-LXC results (for the same ground-state cluster geometry which is optimized) shows the importance of electronic correlation contributions to the absorption spectra.

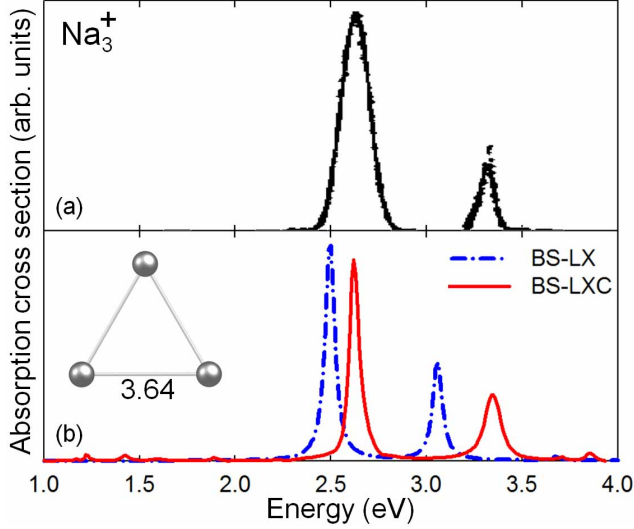


FIG. 2. Experimental and calculated absorption spectra of  $\text{Na}_3^+$ . (a) Experimental spectrum adapted from Ref. 9. (b) Cross section is calculated in the BS-LXC (solid line) and BS-LX (dot-dashed) approximation. The inset shows the cluster structure with the distances in Å.

In Fig. 2 calculated and experimental results are shown for  $\text{Na}_3^+$ . Again, the theoretical spectrum resolves both the larger experimental peak at 2.62 eV as well as the smaller peak at 3.33 eV only when correlations are taken into account. Without correlation contributions, the BS-LX approximation incorrectly describes the positions of the peaks.

In the case of  $\text{Na}_4$ , the BS-LX and BS-LXC approximations yield peaks in the absorption cross section that are energetically close, as can be seen from the panel (b) of Fig. 3. However, the inclusion of correlation effects results in a better agreement with the experimental spectrum shown in panel (a) of Fig. 3, for which the main peaks are centered around 1.8 and 2.5 eV. Panel (c) shows the calculated spectra corresponding to the Lindhard and the BS-L approximation for  $\chi$ . These approximations yield completely different peak positions that are red shifted with about 2 eV. Moreover, the  $f$ -sum rule is not fulfilled for the Lindhard and the BS-L approximations, due to the inconsistency between the single- and the two-particle quantities used.

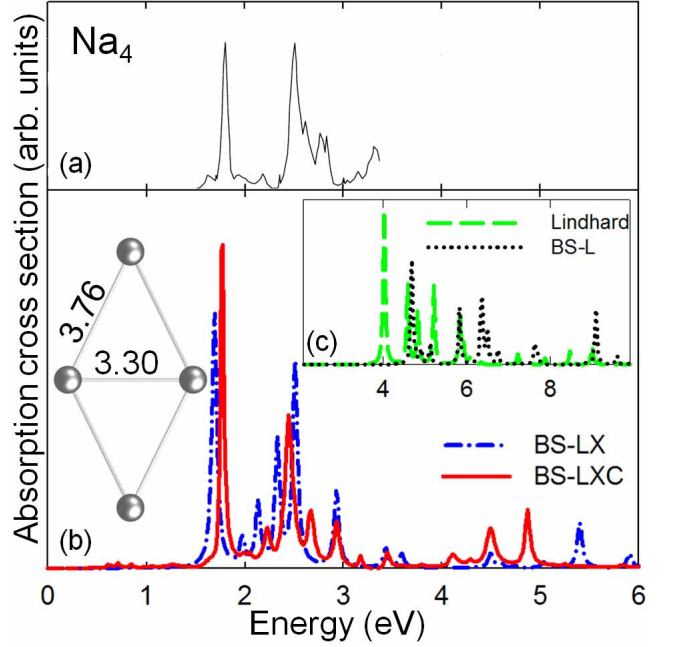


FIG. 3. Experimental and calculated absorption spectra of  $\text{Na}_4^+$ . (a) Experimental spectrum adapted from Refs. 3 and 4. (b) The cross section obtained from the BS-LXC (solid line) and BS-LX (dot-dashed) approximation. The inset shows the cluster structure with the distances in Å. (c) The spectra obtained from the Lindhard (dashed) and BS-L (dotted) approximations.

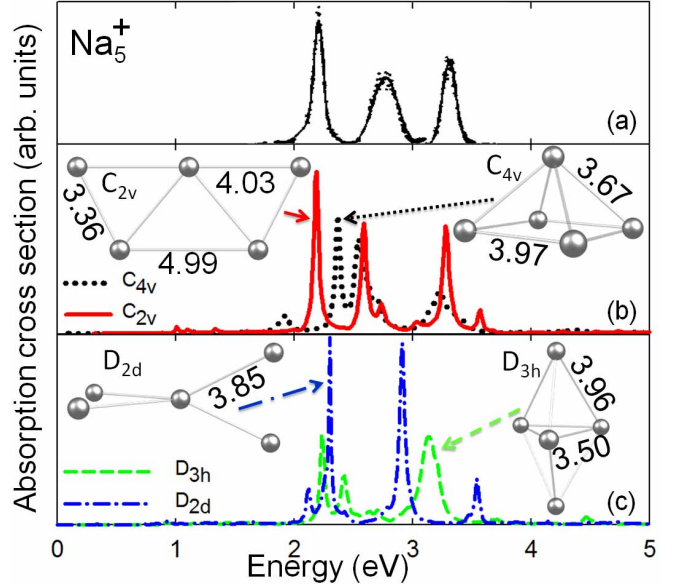


FIG. 4. Experimental and calculated absorption spectra of  $\text{Na}_5^+$ . (a) Experimental spectrum adapted from Refs. 9 and 10. (b), (c) Cross sections in the BS-LXC approximation for clusters with different symmetries:  $C_{2v}$  (solid line),  $C_{4v}$  (dotted),  $D_{2d}$  (dot-dashed), and  $D_{3h}$  (dashed). The insets show the cluster structures with the distances in Å.

To investigate possible geometries of the clusters that

TABLE I. Ground-state total energies (in eV) of the  $\text{Na}_5^+$ ,  $\text{Na}_6$ ,  $\text{Na}_7^+$ , and  $\text{Na}_8$  clusters for several optimized geometrical structures (shown in the panels (b) and (c) of Figs. 4, 5, 6, and 7, respectively). The configuration with the lowest energy corresponds to the most stable geometry.

$\text{Na}_5^+$	$\text{Na}_6$	$\text{Na}_7^+$	$\text{Na}_8$
-21.605 ( $D_{2d}$ )	-29.970 (planar)	-31.866 ( $D_{5h}$ )	-40.121 ( $D_{2d}^{(c)}$ )
-21.476 ( $C_{2v}$ )	-29.821 ( $C_{5v}$ )	-31.329 ( $C_{2v}^{(b)}$ )	-39.934 ( $D_{4d}$ )
-21.168 ( $D_{3h}$ )	-29.526 ( $D_{4h}$ )	-30.984 ( $C_{3v}$ )	-39.661 ( $D_{2d}^{(b)}$ )
-20.526 ( $C_{4v}$ )	-28.937 ( $C_{2v}$ )	-30.829 ( $C_{2v}^{(c)}$ )	-39.934 ( $D_{4d}$ )

may play a role under typical experimental conditions, we consider four different symmetries for  $\text{Na}_5^+$ :  $C_{2v}$ ,  $C_{4v}$ ,  $D_{2d}$ , and  $D_{3h}$ . In Fig. 4 we present spectra calculated in the BS-LXC approximation for each symmetry, and compare them to experiment. As can be seen from the panels (b) and (c) of Fig. 4, the cluster structures which yield the best agreement to the measured cross section correspond to the  $D_{2d}$  and  $C_{2v}$  symmetries. They best resolve the experimental peaks at 2.2, 2.7, and 3.3 eV. The  $D_{2d}$  and  $C_{2v}$  have similar total ground state energies (0.13 eV difference), and are energetically more stable than the  $D_{3h}$  and  $C_{4v}$  structures. In an experiment, at finite temperature, it is possible that both the  $C_{2v}$  and the  $D_{2d}$  clusters are responsible for the shape of the individual peaks, but a clear distinction between the weight of the contribution of each cluster is not possible with a  $T = 0\text{ K}$  theory.

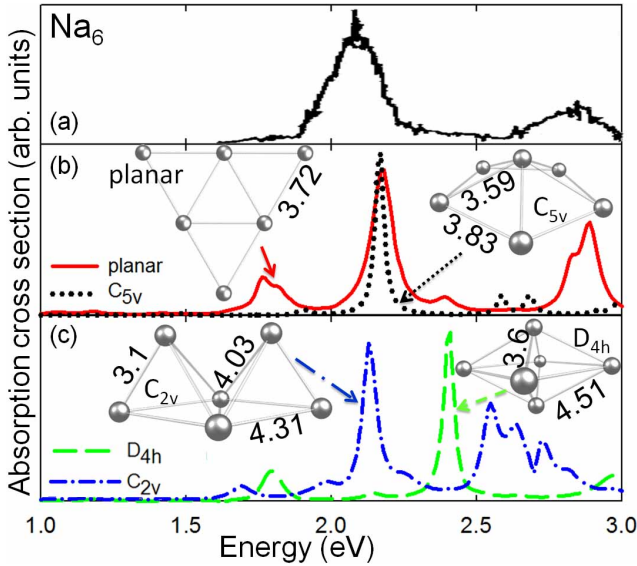


FIG. 5. Experimental and calculated absorption spectra of  $\text{Na}_6$ . (a) Experimental spectrum adapted from Ref. 47. (b), (c) Cross sections in the BS-LXC approximation for clusters with different symmetries: planar (solid line),  $C_{5v}$  (dotted),  $C_{2v}$  (dot-dashed), and  $D_{4h}$  (dashed). The insets show the cluster structures with the distances in Å.

For  $\text{Na}_6$  we have also investigated four different symmetries of the cluster structure: planar,  $C_{5v}$ ,  $C_{2v}$ , and  $D_{4h}$ . From Fig. 5 one can see that the cross section

of the planar and the  $C_{2v}$  geometries agree best with the experimental spectrum. The energetically most stable structure is the planar  $\text{Na}_6$ . The planar structure overestimates by 0.1 eV the position of the dominant experimental peak at 2.1 eV. It resolves the peak around 2.7 eV, but predicts another peak at 1.75 eV, which is not present in the experimental spectrum. In the case of the  $C_{2v}$  cluster, the most prominent peak agrees well with the experimental peak at 2.1 eV, while the position of the smaller experimental peak around 2.7 eV is underestimated by the calculation by 0.2 eV.

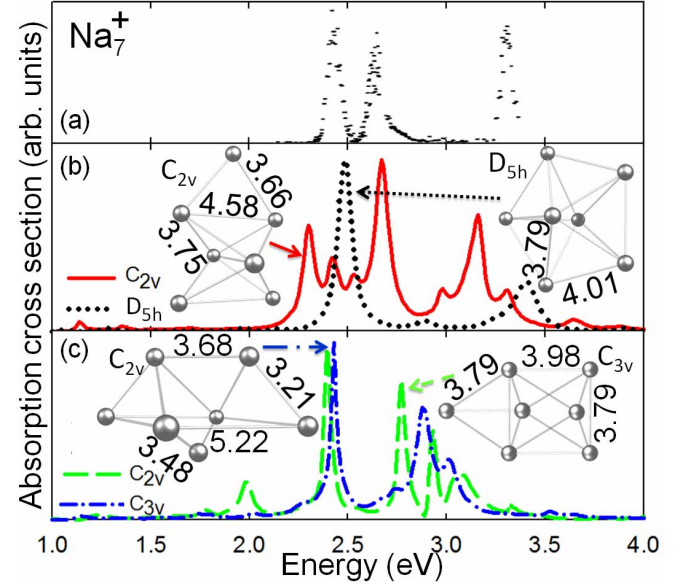


FIG. 6. Experimental and calculated absorption spectra of  $\text{Na}_7^+$ . (a) Experimental spectrum adapted from Ref. 10. (b), (c) Cross sections in the BS-LXC approximation for clusters with different symmetries: two  $C_{2v}$  (solid and dot-dashed lines),  $D_{5h}$  (dotted), and  $C_{3v}$  (dashed). The insets show the cluster geometries with the distances in Å.

In Fig. 6 we show a comparison between the experimental and the theoretical absorption spectra of  $\text{Na}_7^+$ , calculated for two different clusters of  $C_{2v}$  symmetries and also for the  $D_{5h}$  and  $C_{3v}$  geometries. The structure with the most stable energetic configuration is the  $D_{5h}$ , which also reproduces well the 2.4 and 3.3 eV experimental peaks, although with a small offset of 0.1 eV. The experimental peak at 2.4 eV is well reproduced by the structures from panel (c) of Fig. 6, while the  $C_{2v}$  structure from panel (b) resolves well the experimental peak at 2.65 eV.

The measured spectrum of the  $\text{Na}_8$  cluster in Fig. 7 exhibits a single broad peak extending from 2.2 to 2.8 eV. The theoretical result is computed for four different structural symmetries:  $D_{4d}$ ,  $D_{2h}$ , and two different  $D_{2d}$  structures, as shown in Fig. 7. Both the  $D_{4d}$  and the  $D_{2d}$  structures from panel (b) give a pronounced peak around 2.55 eV, which agrees well with the experimental data. However, the  $D_{2d}$  cluster predicts a smaller peak at 2.19 eV not present in the experiment. The  $D_{2d}$  (which



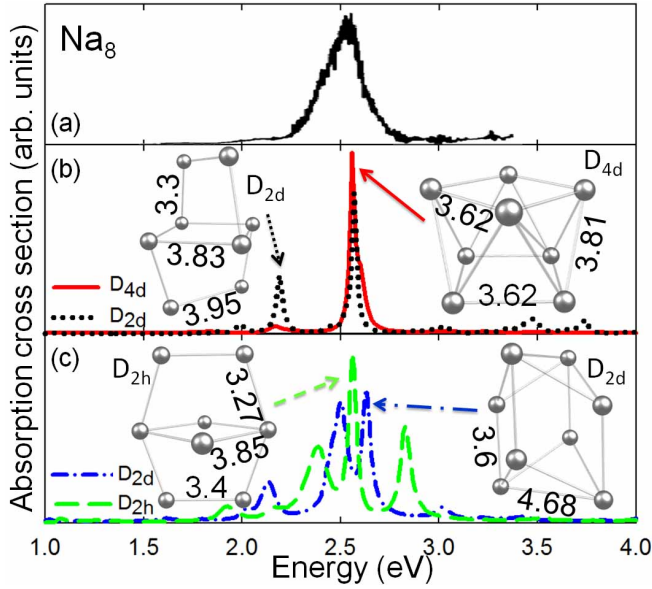


FIG. 7. (color online) Experimental and calculated absorption spectra of  $\text{Na}_8$ . (a) Experimental spectrum adapted from Refs. 3 and 4. (b), (c) Cross sections in the BS-LXC approximation for clusters with different symmetries:  $D_{4d}$  (solid line), two  $D_{2d}$  (dotted and dot-dashed) and  $D_{2h}$  (dashed). The insets show the cluster structures with the distances in Å.

has the lowest ground state energy) and the  $D_{2h}$  structures from panel (c) yield several photoabsorption resonance peaks that lie in the same energy interval as the measured spectra. Therefore, different possible configurations of the cluster geometries and finite temperature might be responsible for the strongly broadened experimental line. However, as mentioned above, it is not possible to assign a clear weight for each individual structure computed for  $T = 0\text{ K}$ . At finite temperatures phonons are present and the eigenmodes of these vibronic states do not only broaden the peaks, but they may also alter the selection rules, leading to new peaks in the absorption spectra<sup>48,49</sup>.

Summarizing, the calculated BS-LXC spectra presented here are in very good agreement with the measured photoabsorption cross sections, given the potential problems for experiment-theory comparisons which are

due to the unknown cluster structures, finite temperature and inhomogeneous broadening effects that tend to wash out the intrinsic spectral features of the resonances.

#### IV. CONCLUSIONS

The absorption spectra of small closed-shell Na clusters were calculated by means of a linear response approach for the electron-hole correlation function, defined as the functional derivative with respect to a weak external perturbation of the non-equilibrium single-particle density matrix. We numerically solved a Bethe-Salpeter-like equation for electron-hole correlation that obeys physical conservation laws by construction. In particular, we numerically checked that the f-sum rule is fulfilled to better than 99%. We found that correlation effects beyond the mean-field limit need to be included in the calculations in order to properly account for the positions and the widths of the resonance peaks. In the present approach, the finite broadening of the photoabsorption lines is attributed to the correlations between the interacting quasielectrons and holes with a finite lifetime.

The computed cross sections of the clusters displayed an overall good agreement with the measured spectra with respect to the positions and the shapes of the photoabsorption lines. For the smaller clusters  $\text{Na}_2$ - $\text{Na}_3$  we found the geometrical configurations that yield theoretical spectra in excellent agreement with the experiment. For the larger clusters  $\text{Na}_5^+$ - $\text{Na}_8$  we have considered different energetically stable geometries, in order to account, within a  $T = 0\text{ K}$  theory, for finite-temperature effects which are unavoidable in experiments. We were able to pinpoint the cluster geometries likely present in the experiments, where the structure cannot be directly obtained.

#### ACKNOWLEDGMENTS

The authors acknowledge support from the German Research Foundation through the Priority Programme 1153. The authors thank Y. Pavlyukh for stimulating and useful discussions.

lefkidis@physik.uni-kl.de

<sup>1</sup> W. D. Knight, K. Clemenger, W. A. de Heer, W. A. Saunders, M. Y. Chou, and M. L. Cohen, Phys. Rev. Lett. 52, 2141 (1984).

<sup>2</sup> W. A. de Heer, K. Selby, V. Kresin, J. Masui, M. Vollmer, A. Chatelain, and W. D. Knight, Phys. Rev. Lett. 59, 1805 (1987).

<sup>3</sup> C. R. C. Wang, S. Pollack, D. Cameron, and M. M. Kappes, J. Chem. Phys. 93, 3787 (1990).

<sup>4</sup> C. R. C. Wang, S. Pollack, D. Cameron, and M. M. Kappes, Chem. Phys. Lett. 166, 26 (1990).

<sup>5</sup> K. Selby, V. Kresin, J. Masui, M. Vollmer, W. A. de Heer, A. Scheidemann, and W. D. Knight, Phys. Rev. B 43, 4565 (1991).

<sup>6</sup> W. A. de Heer, Rev. Mod. Phys. 65, 611 (1993).

<sup>7</sup> T. Reiners, W. Orlik, C. Ellert, M. Schmidt, and H. Haberland, Chem. Phys. Lett. 215, 357 (1993).

<sup>8</sup> C. Ellert, M. Schmidt, C. Schmitt, T. Reiners, and H. Haberland, Phys. Rev. Lett. 75, 1731 (1995).

<sup>9</sup> M. Schmidt and H. Haberland, Eur. Phys. J. D 6, 109 (1999).

<sup>10</sup> M. Schmidt, C. Ellert, W. Kronmüller, and H. Haberland,

- Phys. Rev. B 59, 10970 (1999).
- <sup>11</sup> G. W rigge, M . A stnuc Ho m ann, and B . v. Issendor , Phys. Rev. A 65, 063201 (2002).
  - <sup>12</sup> F. Baletto and R. Ferrando, Rev. Mod. Phys. 77, 371 (2005).
  - <sup>13</sup> K. C km enger, Phys. Rev. B 32, 1359 (1985).
  - <sup>14</sup> D. E. Beck, Phys. Rev. B 30, 6935 (1984).
  - <sup>15</sup> W . Ekardt, Phys. Rev. Lett. 52, 1925 (1984).
  - <sup>16</sup> M . Brack, Rev. Mod. Phys. 65, 677 (1993).
  - <sup>17</sup> S. K um m el, M . Brack, and P.-G . Reinhard, Phys. Rev. B 62, 7602 (2000).
  - <sup>18</sup> C. Yannouleas, R. A . Broglia, M . Brack, and P. F. Bortignon, Phys. Rev. Lett. 63, 255.
  - <sup>19</sup> V. Bonacic-Koutecky, P. Fantucci, and J. Koutecky, Phys. Rev. B 37, 4369 (1988).
  - <sup>20</sup> V. Bonacic-Koutecky, P. Fantucci, and J. Koutecky, Chem . Phys. Lett. 166, 32 (1990).
  - <sup>21</sup> V. Bonacic-Koutecky, P. Fantucci, and J. Koutecky, J. Chem . Phys. 93, 3802 (1990).
  - <sup>22</sup> V. Bonacic-Koutecky, J. P ittner, C. Scheuch, M . F. Guest, and J. Koutecky, J. Chem . Phys. 96, 7938 (1992).
  - <sup>23</sup> V. Bonacic-Koutecky, J. P ittner, C. Fuchs, P. Fantucci, M . F. Guest, and J. Koutecky, J. Chem . Phys. 104, 1427 (1996).
  - <sup>24</sup> A. Rubio, J. A . Alonso, X. Blase, L. C. Balbas, and S. G . Louie, Phys. Rev. Lett. 77, 247 (1996).
  - <sup>25</sup> I. Vasiliev, S. O gut, and J. R. Chelikowsky, Phys. Rev. Lett. 82, 1919 (1999).
  - <sup>26</sup> M . A . L. Marques, A. Castro, and A. Rubio, J. Chem . Phys. 115, 3006 (2001).
  - <sup>27</sup> M . M oseler, H. Hakkinen, and U. Landm an, Phys. Rev. Lett. 87, 053401 (2001).
  - <sup>28</sup> A. Fortini, M . Mazzola, A. Mina, D. Provasi, G. Colb, G. Onida, H. E. Rom an, and R. A . Broglia, J. Phys. B 38, 1581 (2005).
  - <sup>29</sup> J.-O . Joswig, L. O . Tunturivuori, and R. M . Niem inen, J. Chem . Phys. 128, 14707 (2008).
  - <sup>30</sup> G. Onida, L. Reining, R. W . Godby, R. Del Sole, and W . Andreoni, Phys. Rev. Lett. 75, 818 (1995).
  - <sup>31</sup> M . Rohl ng and S. G . Louie, Phys. Rev. B 62, 4927 (2000).
  - <sup>32</sup> G. Onida, L. Reining, and A. Rubio, Rev. Mod. Phys. 74, 601 (2002).
  - <sup>33</sup> M . L. del Puerto, M . L. Tiago, and J. R. Chelikowsky, Phys. Rev. B 77 (2008).
  - <sup>34</sup> M . L. Tiago, J. C . Idrobo, S. O gut, J. Jellinek, and J. R . Chelikowsky, Phys. Rev. B 79, 155419 (2009).
  - <sup>35</sup> L. Hedin, Phys. Rev. 139, A 796 (1965).
  - <sup>36</sup> S. Ishii, K . Ohno, Y . Kawazoe, and S. G . Louie, Phys. Rev. B 63, 155104 (2001).
  - <sup>37</sup> G. Baym and L. P. Kadano , Phys. Rev. 124, 287 (1961).
  - <sup>38</sup> G. Pal, Y . Pavlyukh, H. C . Schneider, and W . Hubner, Eur. Phys. J. B 70, 483 (2009).
  - <sup>39</sup> G. Pal, Y . Pavlyukh, W . Hubner, and H. C . Schneider, unpublished (2009).
  - <sup>40</sup> Y . Pavlyukh, J. Berakdar, and W . Hubner, Phys. Rev. Lett. 100, 116103 (2008).
  - <sup>41</sup> Y . Pavlyukh and W . Hubner, Phys. Lett. A 327, 241 (2004).
  - <sup>42</sup> P. J. Hay and W . R. W adt, J. Chem . Phys. 82, 270 (1985).
  - <sup>43</sup> A. K . Rappe, T. Sm edly, and W . A . G oddard III, J. Phys. Chem . 85, 1662 (1981).
  - <sup>44</sup> W . Stevens, H. Basch, and J. K rauss, J. Chem . Phys. 81, 6026 (1984).
  - <sup>45</sup> P. Fuentealba, H . Preuss, H . Stoll, and L. v. Szentpaly, Chem . Phys. Lett. 89, 418 (1989).
  - <sup>46</sup> W . R. Fredrickson and W illiam W . W atson, Phys. Rev. 30, 429 (1927).
  - <sup>47</sup> C. R. C. W ang, S. Pollack, T. A . Dahlseid, G. M . Koretsky, and M . M . Kappes, J. Chem . Phys. 96, 7931 (1992).
  - <sup>48</sup> G. Lefkidis, O . Ney, and W . Hubner, phys. stat. solidi (c) 12, 4022 (2005).
  - <sup>49</sup> G. Lefkidis and W . Hubner, Phys. Rev. B 74, 155106 (2006).
  - <sup>50</sup> N. E. Dahlen and R. van Leeuwen, Phys. Rev. Lett. 98, 153004 (2007).
  - <sup>51</sup> K. S. Thygesen and A. Rubio, Phys. Rev. B 77, 115333 (2008).
  - <sup>52</sup> J. Ram mer and H . Sm ith, Rev. Mod. Phys. 58, 323 (1986).
  - <sup>53</sup> P. Lipavsky, V . Spicka, and B. Velicky, Phys. Rev. B 34, 6933 (1986).
  - <sup>54</sup> G. Baym , Phys. Rev. 127, 1391 (1962).
  - <sup>55</sup> S. Ismail-Beigi and S. G . Louie, Phys. Rev. Lett. 90, 076401 (2003).
  - <sup>56</sup> D. K rem p, M . Schlages, and W .-D . K raef, Quantum Statistics of Nonideal Plasmas (Springer, Berlin Heidelberg New York, 2005).